Cell Reports, Volume *42*

Supplemental information

All-optical recreation of naturalistic neural activity with a multifunctional transgenic reporter mouse

Hayley A. Bounds, Masato Sadahiro, William D. Hendricks, Marta Gajowa, Karthika Gopakumar, Daniel Quintana, Bosiljka Tasic, Tanya L. Daigle, Hongkui Zeng, Ian Antón Oldenburg, and Hillel Adesnik

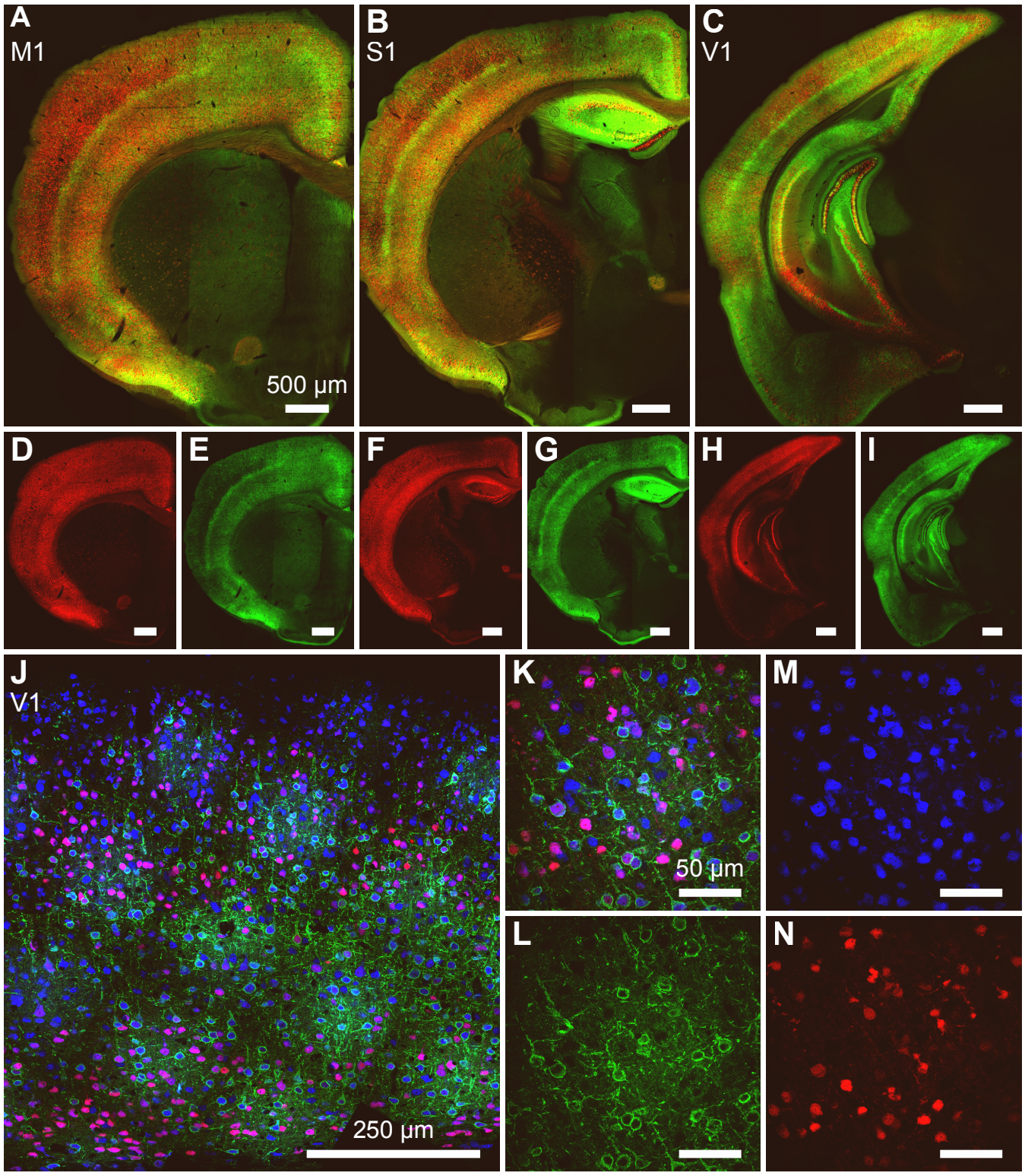

Figure S1: Expression of nls-mRuby3 and GCaMP7s in Vglut1-Cre;Ai203, related to Figure 1.
A-I: Confocal images of brain sections from Vglut1-Cre;Ai203 mice showing expression of st-ChroME-GCaMP7s (green) and nls-mRuby3 (red) (images stitched from multiple fields of view). A-C, composite images of both mRuby3 and st-ChroME-GCaMP7s. D-I, sections in A-C separated by channel.
J: One of five areas used for quantification of expressing cells, showing anti-NeuN (blue), nls-mRuby3 (red), st-ChroME-GCaMP7s (green). Area is composed of stitched fields of view taken at high magnification for optical sectioning, then rotated and cropped to get a full depth section.
K-N: one example field of view from the area in J. K: composite, M: anti-NeuN, L: st-ChroME-GCaMP7s, N: nls-mRuby3.

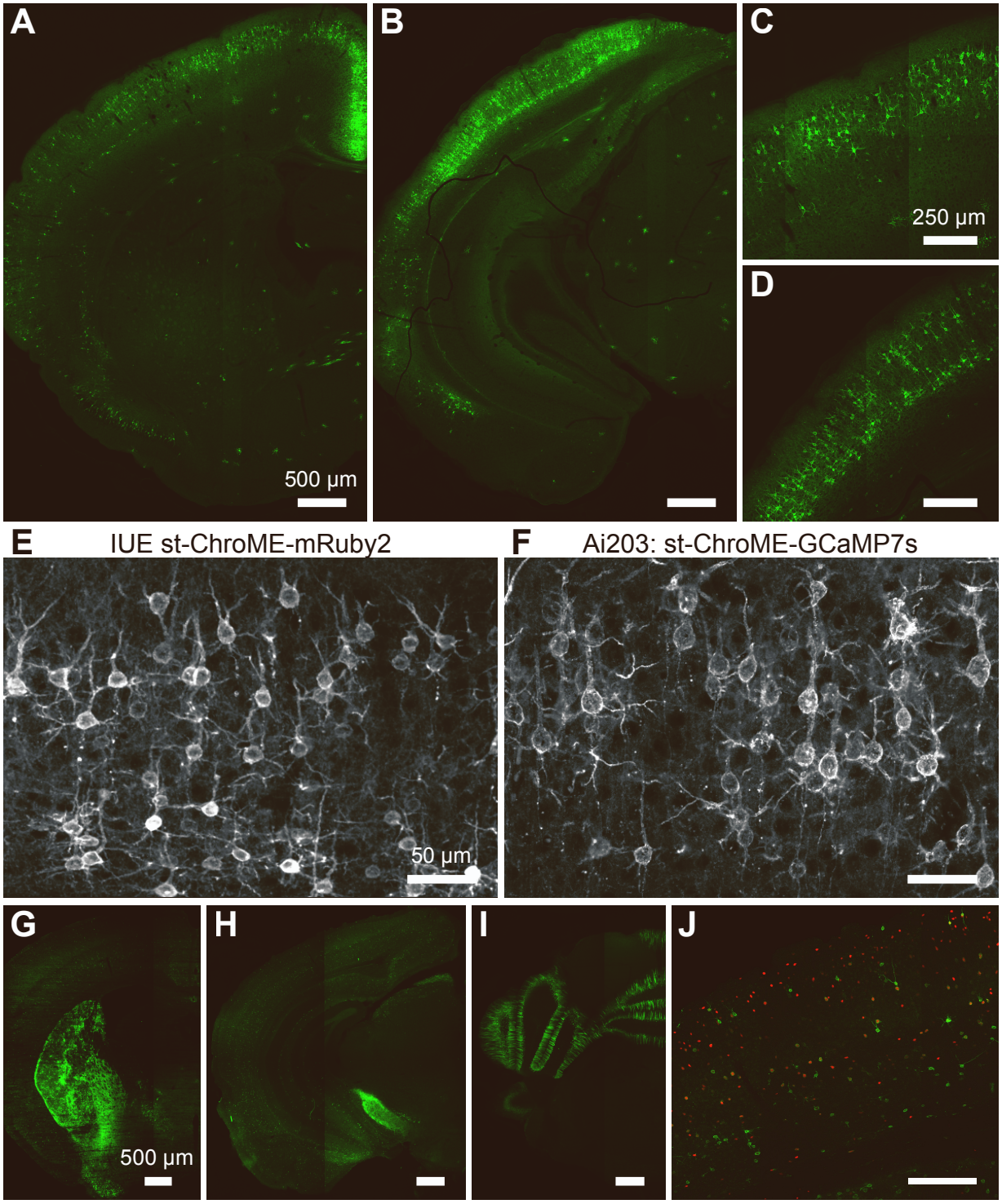

Figure S2: Expression of GCaMP7s and nls-mRuby3 in Cux2-CreERT2;Ai203 and Vgat-IRES-Cre;Ai203 mice, related to Figure 1.

A-D: Confocal images of post-mortem tissue from one example Cux2-CreERT2;Ai203 mouse at two different coronal sections and two zooms showing st-ChroME-GCaMP7s expression in green (images stitched from multiple fields of view). A,C: primary motor cortex, B,D: primary visual cortex

E-F: Comparison of in utero electroporation st-ChroME-mRuby2 to transgenically expressed st-ChroME-GCaMP7s in Cux2-CreERT2;Ai203.

G-J: Confocal images of post-mortem tissue from one example Vgat-IRES-Cre;Ai203 mouse at different coronal sections showing st-ChroME-GCaMP7s expression in green (images stitched from multiple fields of view). G: section containing motor cortex and striatum, H: section containing primary visual cortex, I: section of the cerebellum. J: section showing visual cortex.

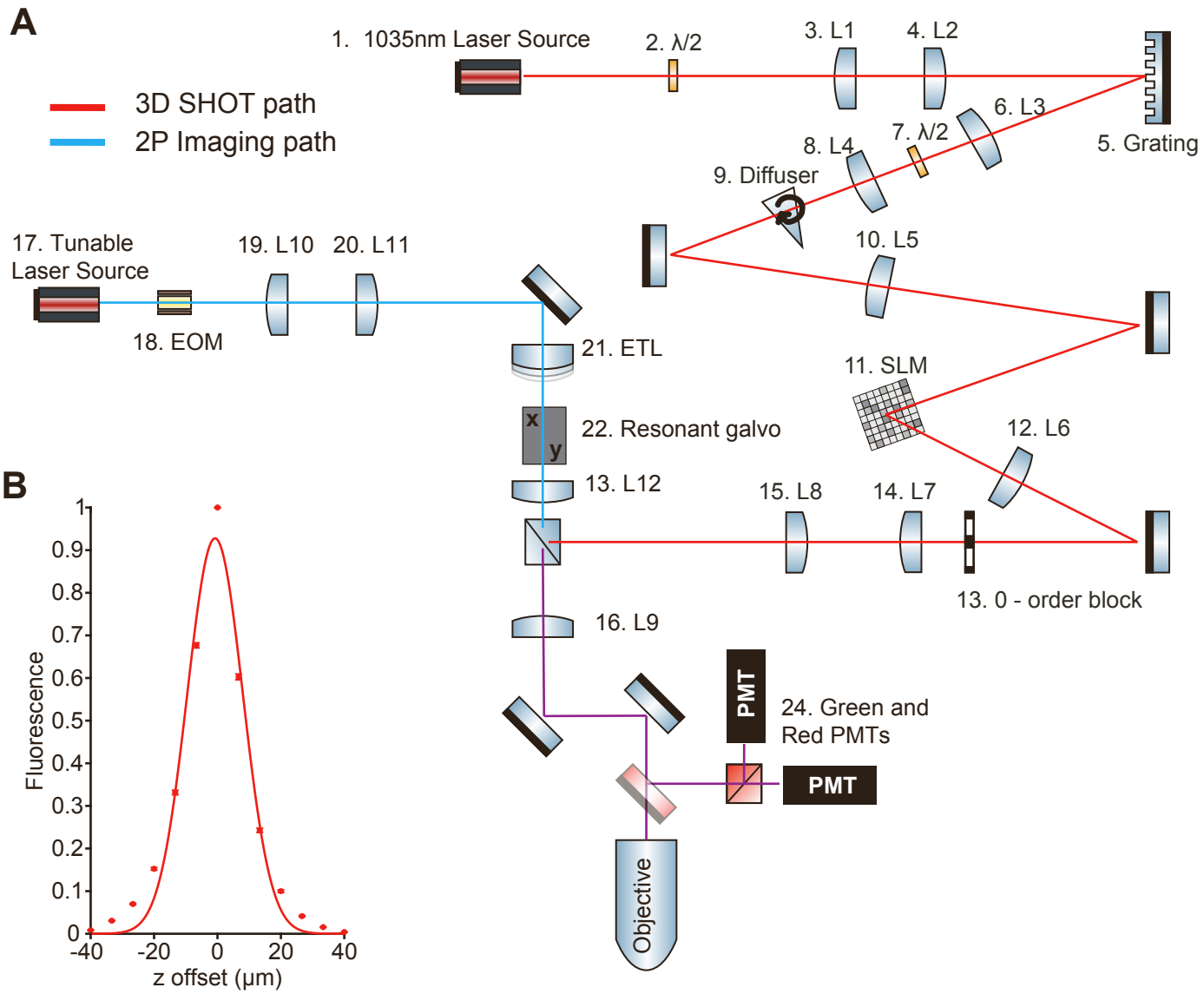

Figure S3: Optical path for combined 2-photon imaging and holographic optogenetics, related to STAR Methods.

A: Schematic of combined 2-photon imaging and holographic photostimulation (3D-SHOT) paths for Setup #1 (see Supplementary Table 1 and methods for details). Components 1-15 (red beam line) correspond to the 3D-SHOT path and components 17-22 (blue beam line) correspond to the 2-photon imaging path. The imaging path and photostimulation path are combined before the tube lens (element 16) with a polarizing beam splitter. Component 16 and the objective are shared by the combined imaging and 3D-SHOT path (purple beam line). Dichroic mirrors and PMTs are used in the 2-photon imaging collection path (red and green beam lines). Abbreviations: L: lens, SLM: spatial light modulator, EOM: electro-optical modulator (Pockels cell), ETL: electrically tunable lens, PBS: polarizing beam splitter, PMT: photomultiplier tube.

B: Axial (z) resolution of the average of 1110 measured holograms in Setup #1 measured by a camera capturing intensity on a fluorescent slide. FWHM: 20.7 μm. Data are shown as mean ± sem.

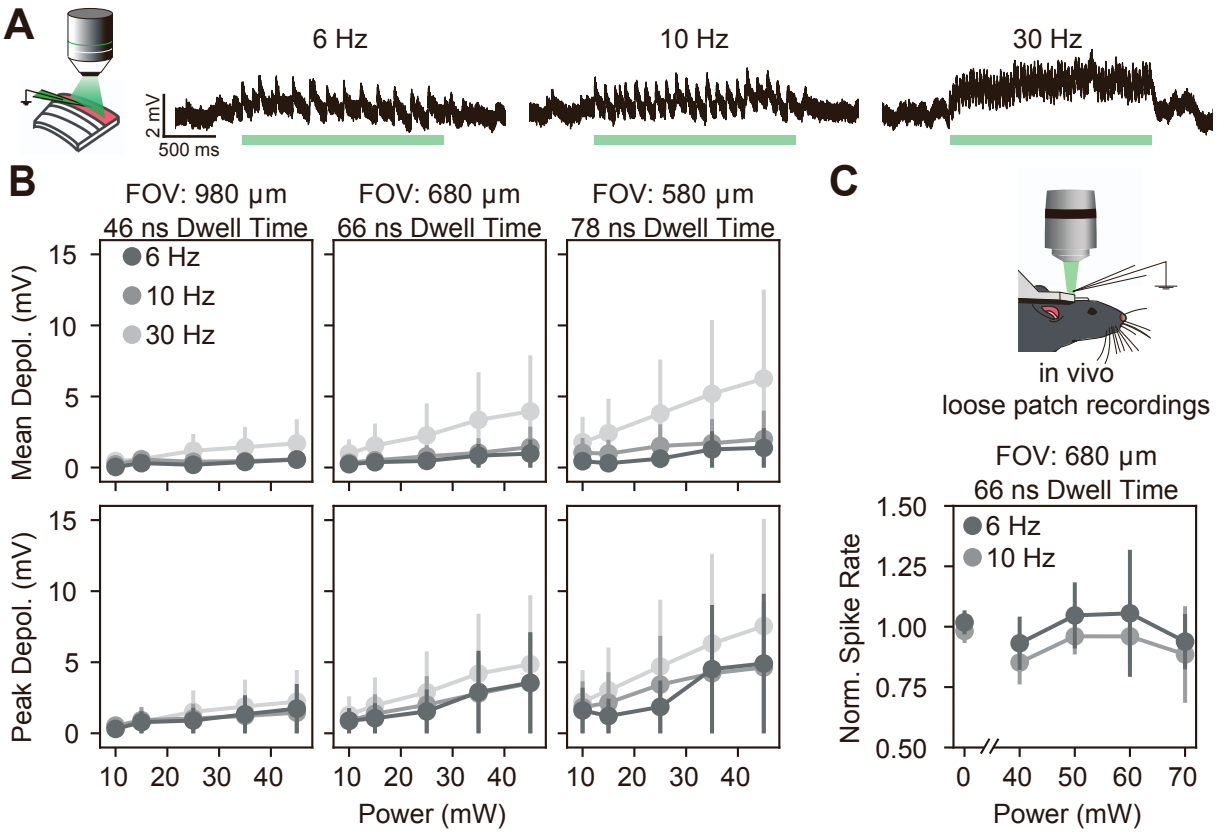

Figure S4: 2p scanning-evoked activation in vitro and in vivo, related to Figure 1.
A: Left, schematic of the experimental setup. Whole-cell recordings were made during 2p imaging with different imaging rates, powers, and scanning field of view (FOV) sizes. Scanning-induced depolarization, or "cross talk," was recorded. Right, three example traces from one cell recorded at different frequencies, all with 45 mW imaging power and a 980 µm FOV.
B: Mean (top) and peak (bottom) depolarization during 2p imaging of opsin-positive neurons. From left to right, increasing zoom and decreasing field of view size, and increasing dwell times (FOV 980: 46 ns/µm; FOV 680: 66 ns/µm; FOV 580: 78 ns/µm).
C: Crosstalk measurements in vivo. Normalized spike rates without imaging (0 power) and with imaging at different powers and imaging rates. Effect of power: p=0.88, effect of imaging rate: p=0.24, effect of power x imaging rate: p=0.99, repeated measures ANOVA, n=4 cells).
Data are shown as mean ± sem.

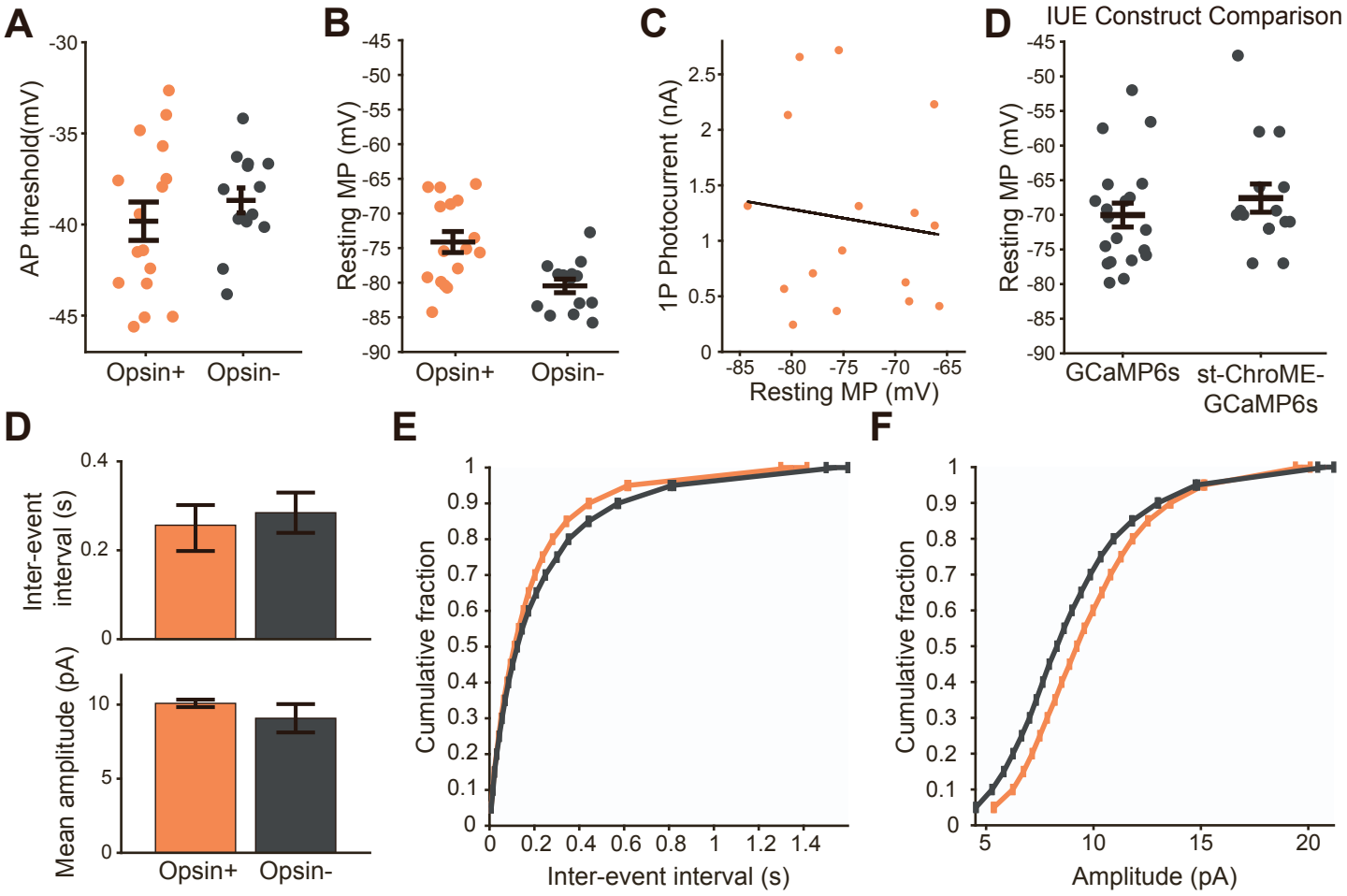

Figure S5: Comparison of basic physiological and synaptic properties of opsin+ and opsin- neurons in Ai203 mice, related to Figure 2.

A: Action potential (AP) threshold, measured by electrical stimulation, for opsin+ and opsin- neurons, categorized based on 1p photocurrent (p=0.53; n=16 cells for opsin+ and n=14 for opsin-; t-test).

B: Resting membrane potential (MP) for the cells in A (p=.002, n=16 cells for opsin+ and n=14 for opsin-; t-test)

C: Magnitude of 1p photocurrent vs resting membrane potential for cells in A (slope=-.016, R2 0.014, p=.66 that slope is different than 0)

D: Data from animals with in utero electroporation (IUE) of either a GCaMP6s or st-ChroME-GCaMP6s construct showing resting membrane potential (p=0.364; t-test; n=20 cells for GCaMP6s and n=15 cells for st-ChroME-GCaMP6s).

E: Comparison of miniature excitatory post-synaptic currents (mEPSCs) in opsin positive and opsin negative cells. Top, inter-event intervals between mEPSCS, bottom, mean amplitude of mEPSCs.

F: Cumulative distribution of interevent intervals between opsin+ and opsin- cells (p<0.0001, KS test. n=8 cells).

G: Cumulative distribution of mEPSC amplitude between opsin + and opsin – cells (p<0.0001, KS test, n=8 cells).

Data are shown as mean ± sem.

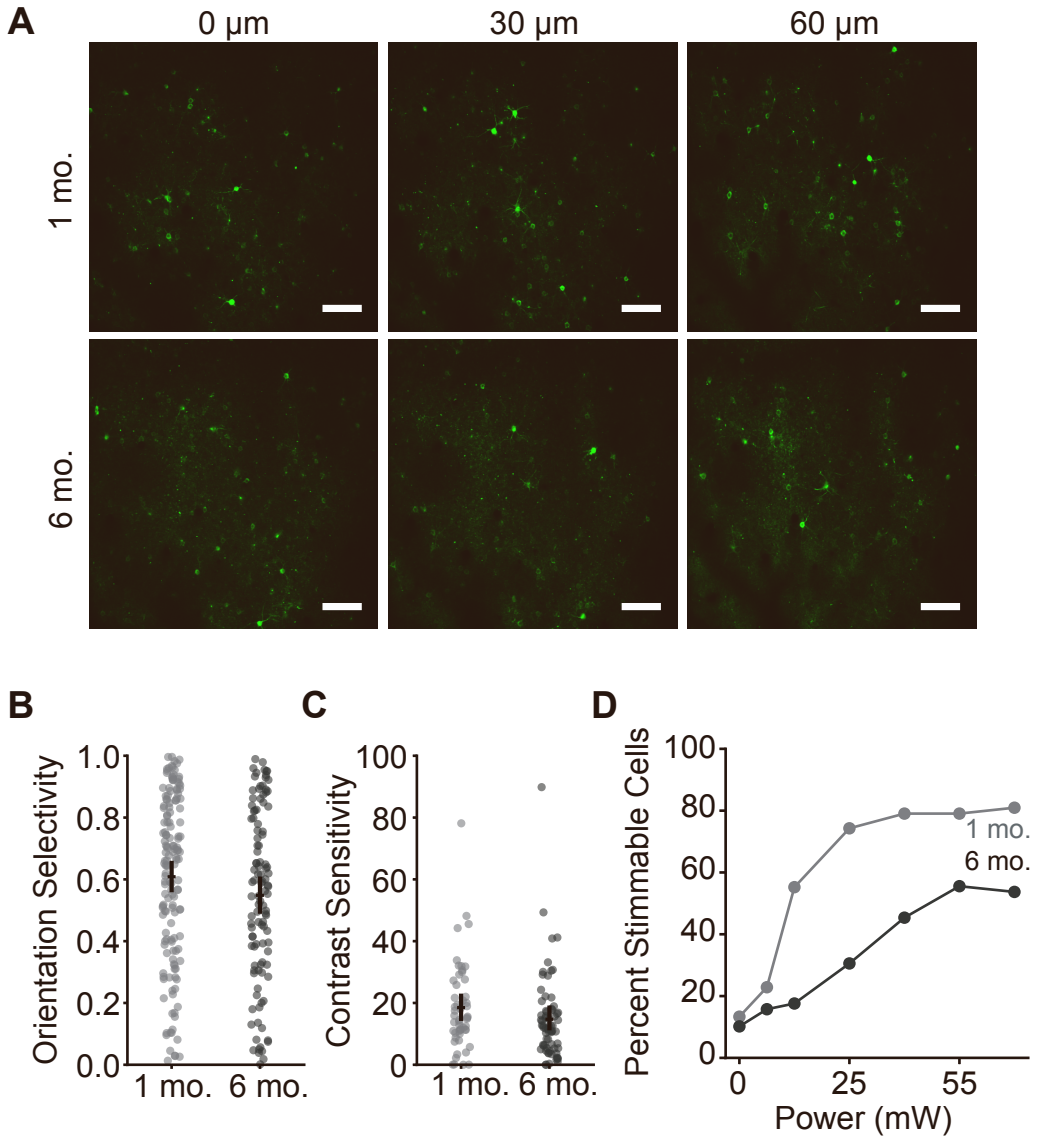

Figure S6: Long-term transgene expression in Ai203 mice, related to Figure 2.
A: in vivo images from a matched field-of-view (FOV) from a single Ai203 mouse captured at 3 different z-planes (columns; 0, +30, +60 µm) at 1-month post-windowing (top row) and 6-months post-windowing (bottom row). Scale bar, 100 µm.
B: Comparison of orientation selectivity (orientation selectivity index, OSI) measured at 1-month (left, light grey) and 6-months (right, dark grey) post-windowing for matching FOVs. OSI: 1-month, 0.61 ± 0.02, n=152 cells; 6-months, 0.55 ± 0.03, n=110 cells.
C: Comparison of contrast sensitivity (C50, Naka-Rushton fit) measured at 1-month (left, light grey) and 6 months (right, dark grey) post-windowing for matching FOVs. C50: 1-month, 18 ± 2%, n=52 cells; 6-months, 15 ± 2%, n=68 cells.
D: Quantification of percent neurons activated at various powers between 1-month (light grey) and 6-month timepoints (percent activatable at 70 mW: 1-month, 81%, 6-month, 54%).

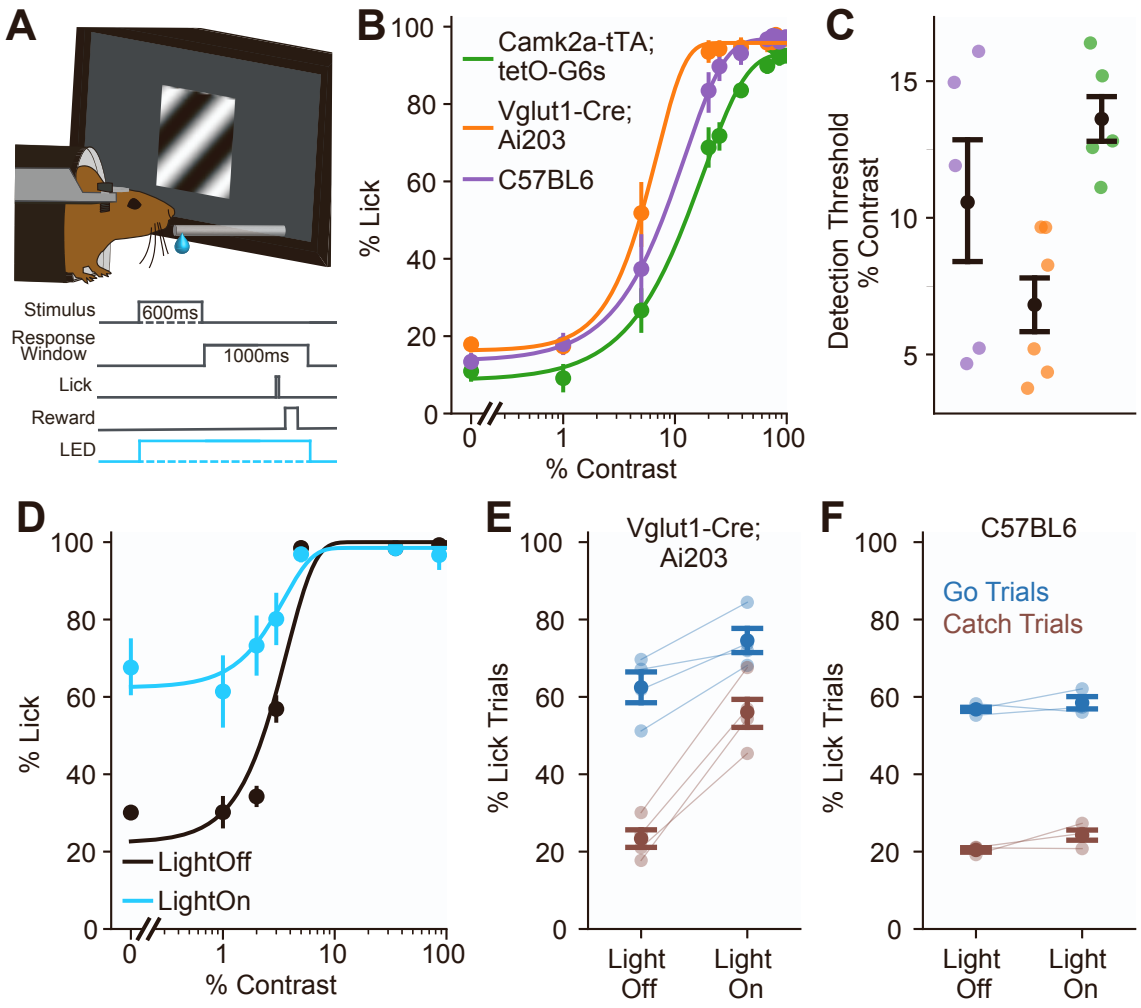

Figure S7: Optogenetic manipulation of operant behavior in Vglut1-Cre;Ai203 mice alters performance, related to Figure 2.

A: Schematic of the visual detection task. Gratings of varying contrasts were presented to mice trained to lick during a 1 second response window following stimulus presentation to indicate detection.

B: Psychometric curves averaged across mice for of the three strains tested. n=6 mice for Vglut1-Cre;Ai203, n=5 each for wildtype and Camk2a-tTA;teto-GCaMP6s.

C: Comparison of detection threshold across genotypes, points are individual mice. p=0.004, one-way ANOVA, with post-hoc Tukey test: Ai203 vs wt p=0.31; Ai203 vs Camk2a p=0.0046; Camk2a vs wt p=0.21; n=16 mice

D: Psychometric curves averaged across four sessions from one example mouse with (blue) and without (black) 1p stimulation at 470 nm of V1.

E: Comparison of performance metrics with and without 1p stimulation for Vglut1-Cre;Ai203 mice. Hit (blue) and False Alarm (brown) rates (hit rate: p=0.019, false alarm rate: p=0.0016, paired t-test, n=4 mice). Points are individual mice, average of four sessions per mouse.

F: Comparison of performance metrics with and without 1p stimulation for wildtype mice. Hit (blue) and False Alarm (brown) (hit rate: p=0.51; false alarm rate: p=0.25; paired t-test; n=3 mice). Points are individual mice, average of four sessions per mouse.

Data are presented as mean ± bootstrapped 68% confidence interval.

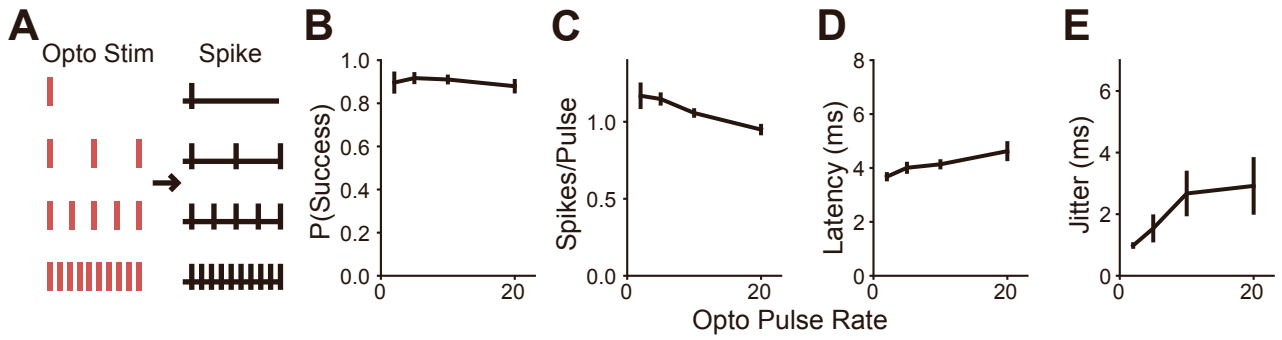

Figure S8: Statistics on spiking for Ai203 cells recorded in vivo, related to Figure 3.
A: Schematic of experiment showing how pulse number and stimulation rate vary together.
B: P(Success), defined as the chance that a single pulse evokes at least one spike, for varying pulse numbers/rates (n=11 cells).
C: Spikes/pulse, the average number of spikes elicited by a single pulse, for varying pulse numbers/rates (n=11 cells).
D: Latency, the time from the start of a 5 ms pulse to the first spike, for varying pulse numbers/rates (n=11 cells).
E: Jitter, the standard deviation of the latency, for varying pulse numbers/rates (n=11 cells).
Data are shown as mean ± sem.

Supplementary Table 1: Details of microscope optics

Lens #	Focal Distance, Setup #1	Focal Distance, Setup #2	Path
L1	80	-	3D SHOT
L2	500	-	3D SHOT
L3	200	100	3D SHOT
L4	40	20	3D SHOT
L5	500	500	3D SHOT
L6	200	200	3D SHOT
L7	250	200	3D SHOT
L8	200	200	3D SHOT
L9	180	180	MOM tube lens
L10	30	75	Imaging path
L11	60	100	Imaging path
L12	50	50	Scan lens